한국부식학회지
J. Corros Sci. Soc. of Korea
Vol. 27 No. 1, February, 1998
〈연구논문〉

Effect of Yttrium on the Sulfidation Behavior of Alloy 690

C. K. Rhee, J. Jang, I. H. Kuk, M. Ritchie* and A. Mitchell*

Korea Atomic Energy Research Institute(KAERI)

150 Dukjin-dong, Yusong-gu, Taejon, 305-353, Korea

**University of British Columbia, Vancouver, B.e , V6T 1Z4, Canada*

Thermally treated(TT) Alloy 690 and Alloy 690-0.1wt.% Y were sulfidized at 900℃ in flowing gas mixtures of Ar, CO_2 and SO_2 for various times and mechanical and microstructural analyses were made. It was found that the microstructure and recrystallization temperature of both alloys remained unchanged, whereas the grain growth and tensile properties were slightly changed by yttrium addition and that the isothermal sulfidation rate of Alloy 690 was reduced by the addition of 0.1wt.% yttrium. SEM and EDX analyses showed that mainly Cr_2O_3 with a small amount of CrS scale was formed on Alloy 690, whereas more complex scales were formed on Alloy 690-0.1wt.% Y because of the non-uniform distribution of yttrium on the matrix in flowing Ar-10% CO_2-2% SO_2. Continuous CrS scales were formed on both yttrium bearing and yttrium free alloys in flowing Ar-10% CO_2-4% SO_2 in the early stage of sulfidation, but after a longer period of sulfidation, a mixed CrS and (Ni,Fe)S outer layer was found. Spallation at the interfaces between CrS and mixed CrS-(Ni,Fe)S, sulfur segregation on yttrium-rich phases and oxide scale refinement were observed and pegging by the yttrium-rich phase was also found.

Keywords : yttrium, high temperature sulfidation, nickel base alloy, sulfur getter, oxide.

1. Introduction

Because of its improved high temperature corrosion resistance and mechanical properties, the alloy 690 has been used as replacement material for steam generator tubes of nuclear power plants replacing the alloy 600 which has suffered various corrosion problems such as SCC, pitting and high temperature corrosion.[1] For over 30 years, many researches have been conducted to improve the high temperature corrosion behaviour of Fe-Ni-Al alloys and Ni-Cr alloys by the addition of small amounts of reactive elements such as yttrium and lanthanum. Several alloys have already been commercialized.

The protection of these nickel base alloys against high temperature oxidation(or sulfidation) is usually provided by the selective oxidation(or sulfidation) of chromium or aluminium to form a compact, adherent and slow-growing protective scale, and it is well known that a small yttrium addition improves the adhesion of protective scales and gives excellent oxidation resistance to many alloys. Although many mechanisms explaining the beneficial effect of this reactive element have been proposed,[2-15] the role

of yttrium in alloys has not yet been thoroughly evaluated. Recently, Schumann et al.[2] released the report of their direct observations of yttrium and sulfur interaction, and their results supported the sulfur effect model. The possible models which can explain the beneficial effect of yttrium addition on oxidation behavior are the following two ways, the change of oxide growth rate and the adherence of the protective scale.

For the first model, several different mechanisms have been proposed. Giggins and Pettit[6] proposed that yttria particles incorporate into the oxide scale and effectively decrease the volume available for chromium diffusion. In contrast, Stringer et al.[7] suggested that yttrium greatly reduces the oxide grain size and that the principal role of yttrium is to act as physical discontinuities, nucleating oxide in the early stage of oxidation. Cotell et al.[8] proposed the transport mechanism which is changed from a predominantly chromium cation outward diffusion to an anion inward diffusion, and concluded that the strain induced segregation of yttrium at the grain boundaries of the oxide reduces the cation flux along the grain boundaries. Ramanarayanan[9] believed that yttrium dopes into the chromium oxide scale as a donor, decreases the number of chromium interstitials, and thereby suppresses transport of chromium.

Concerning the second model, pegging is the most frequently reported mechanism. Many researchers have proposed that yttrium can promote the formation of oxide intrusions into the metal substrate which are supposed to pin the oxides and suppress their spallation.[11] Additionally, yttrium can act as a preferred site for the nucleation of vacancies that would otherwise form at the oxide-metal interface and lead to scale spallation.[12] In contrast, Smeggil[13,14] proposed that yttrium can getter the sulfur and suppress its segregation to the oxide-metal interface to prevent a weakening of the interfaces.

The purpose of this work was to study the sulfidation behaviour of Alloy 690 with the addition of 0.1wt.% yttrium to evaluate the various proposed mechanisms relating to both oxide scale growth and oxide scale adherence. Sulfidation kinetics, microstructure and microchemistry of the scale have been investigated in detail.

2. Experiment

The alloy compositions used in this study are shown in Table 1 and were provided by the courtesy of Inco Alloy International Inc. Huntington, VA. All of these alloys were melted by vacuum induction and supplied in the hot rolled form of 5 to 8mm thickness. It was cold rolled to a 1mm thickness and solution heat-treated in the temperature ranges of 600 to 1110℃ and then thermally treated at 725℃ for 10 hr in order to get an enhanced grain boundary carbide precipitation. The amounts of recrystallization and grain growth were measured by the microhardness and microstructure. Subsize tensile test specimens were machined according to ASTM E8 and tested in the cross head speed of 3mm/min at room temperature. The sulfidation specimens were polished through several grades of SiC abrasion paper, ending at 1 μm diamond paste on a polishing cloth. A platinum wire of 0.5mm diameter was spot-welded on the sample surface to suspend the sample within a furnace. The samples were sulfidized at 900℃ in flowing gas mixtures of SO_2, CO_2 and Ar which passed through a heated carbon powder bath(750℃) be-

Table 1. Chemical composition of Alloy 690 and 690 with Y

wt.%

	Ni	Cr	Fe	Si	Mn	P	Ti	Y	C	S	O	N
Alloy 690	bal.	29.9	9.4	0.15	0.17	60ppm	0.28	0.0	0.018	<0.001	N/A	N/A
Alloy 690+0.1Y	bal.	29.9	9.2	0.08	10ppm	81ppm	0.27	0.07	0.018	<0.001	0.0035	0.0055
Alloy 690+0.1Y+0.05S	bal.	29.9	9.2	0.09	10ppm	73ppm	0.28	0.07	0.02	0.035	N/A	N/A

fore entering into the furnace. The specimens were suspended in the furnace for various times up to 100 hr and then air cooled to room temperature. The gas mixtures selected were Ar-10% CO_2, Ar-10%CO_2-2%SO_2 and Ar-10%CO_2-4% SO_2. Ar and CO_2 gas mixtures were used to lower the oxygen partial pressure. A microbalance was used to follow the weight change during sulfidation. Scanning electron microscope (SEM) with EDX was used to analyze the topography of the sulfidation scale and cross-section of the specimen, which was metallographically mounted, polished and etched with 5% nital or 2 % bromine-methanol.

3. Results and Discussion

The microstructures of both the Alloy 690 and Alloy 690-0.1wt.%Y after 1110℃, 15 min solution annealing followed by 725℃, 10 hr thermal treatment are shown in Fig. 1. Both alloys showed the same microstructure, with a grain size of about 70㎛, regardless of yttrium addition. Table 2 shows the tensile test results of both Alloy 690 and Alloy 690 with yttrium after solution annealing and thermal treatment. The YS and UTS of Alloy 690 increased slightly, whereas its elongation decreased by 5% with a small addition of yttrium. Fracture surface analyses showed no difference on fracture morphology between the two alloys. It was reported[12] that the yttrium which precipitates at the grain boundaries pin the misfit dislocations to make them

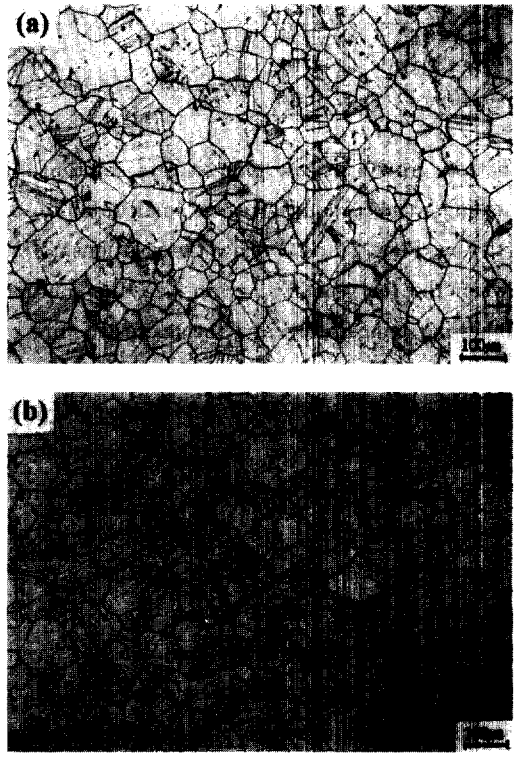

Fig. 1. Typical microstructures of Alloy 690 (a) and Alloy 690-0.1wt.% Y (b) after 1100℃ 15 min solution annealing and 720℃ 10hr thermal treatment(TT).

less mobile which probably increases the YS and UTS and decreases elongation, thereby possibly affecting the oxidation rate by blocking the cation vacancy annihilation process. It was also found that recrystallization occurred at the same temperature of 650℃ in both alloys and that there was no clear effect on the recrystallization temperature by a yttrium addition, whereas there was some retardation ef-

Table 2. Room temperature tensile test results of Alloy 690 and 690 with yttrium

		YS (MPa)	UTS (MPa)	E.L (%)	Remark
MA (1100℃, 15min)	Alloy 690	428	785	39.3	Ave. of 3
	Alloy 690 +0.1wt.%Y	446	795	35.6	〃
MA+TT (MA+725℃ 10hr)	Alloy 690	420	781	40.9	〃
	Alloy 690 +0.1wt.%Y	448	805	36.4	〃

fect on growth at low temperature solution annealing in accordance with a small addition of yttrium. Figs. 2 and 3 show the relationship between the recrystallized grain size, the solution annealing temperature and the microstructure of the Alloy 690-0.1wt.%Y after low temperature solution annealing (920℃, 2 hr), respectively. In Fig. 3, it was observed that the distribution of the grain size was non-uniform and that yttrium could be found at the grain boundaries in the region with small grains, indicating that yttrium had precipitated on the grain boundaries of small grains non-uniformly and blocked grain growth. Figs. 4-(a) and (b) are the SEM-EDX results which show a high yttrium concentration on the grain boundaries.

Another form of yttrium found in the yttrium containing alloy is a spherical type YAl_xO_y oxide sized around 2 to 5μm. Fig. 5-(a) shows the typical form of a yttrium-rich oxide which had formed relatively uniformly in both the matrix and grain boundaries. It has been generally known[7] that yttrium is present mainly as an oxide dispersed in the metal and could affect the oxidation behavior by greatly improving the scale adhesion. However, it is not clear which type of yttrium phase between the yttrium precipitated at the grain boundaries and the yttrium oxide is dominant. The results of X-ray

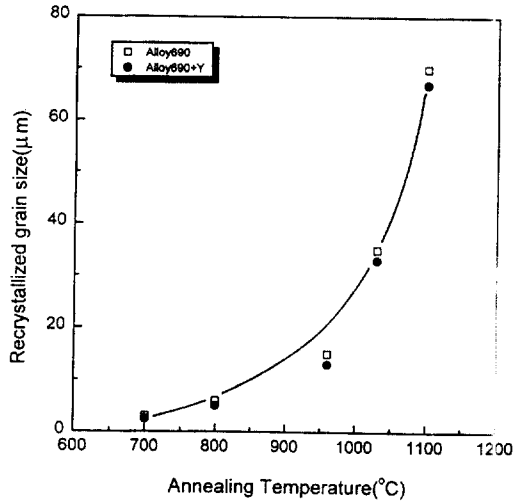

Fig. 2. Relationship between recrystallized grain size and solution annealing temperature.

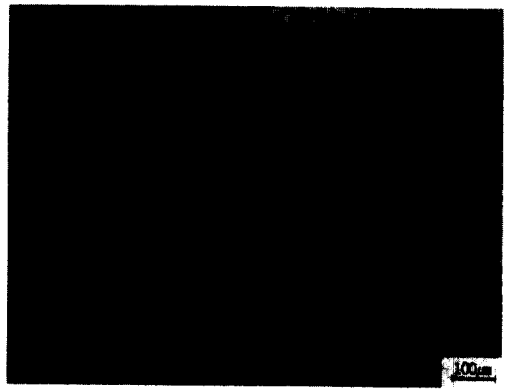

Fig. 3. Microstructure of Alloy 690-0.1%Y after low temperature annealing(920℃, 2hr).

mapping of yttrium and sulfur on the YAl_xO_y oxide by SEM-EDX are shown in Figs. 5-(b) and (c). It was found that these yttrium-rich oxides contained more sulfur(Fig. 5-(c)) in the Alloy 690-0.1wt.% Y-500ppm S, which strongly suggests that yttrium can getter the sulfur from the matrix and prevent it from segregating into the metal-scale interface. However, it has not been found that sulfur segregated to the metal/oxide interface in the yttrium free alloy to

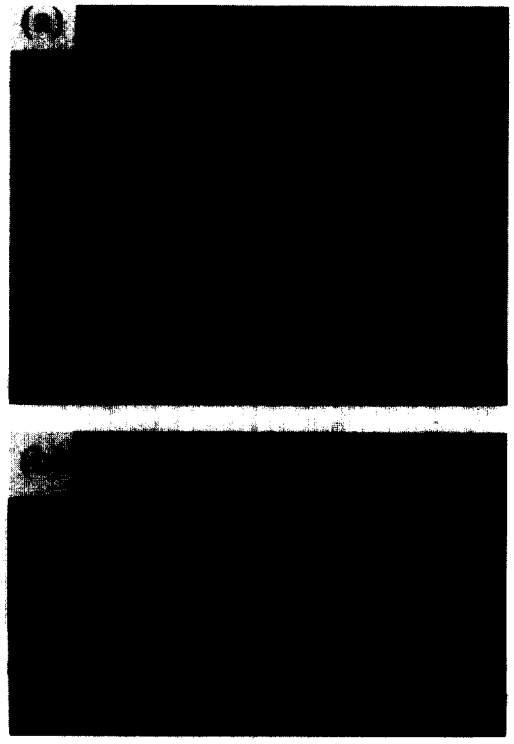

Fig. 4. Microstructure of small grained region(a) and EDX line scan of yttrium(b).

weaken the bonding in this study yet.

Sulfidation kinetics studies were performed at 900℃ for duration of 1~60 hr under various SO_2 partial pressures. The gas mixtures selected were Ar-10%CO_2, Ar-10%CO_2-2%SO_2 and Ar-10%CO_2-4%SO_2. During this period, the parabolic rate law was found to be obeyed throughout the whole experiment by both the Alloy 690 and Alloy 690-0.1wt.%Y, implying that oxide growth occurs by diffusional transport through the scale. The results are shown in Fig. 6. It was observed that the isothermal sulfidation rate of Alloy 690 was reduced by about a factor of 2 with the addition of 0.1wt.% yttrium and that the sulfidation rate increased with increasing SO_2 gas content in both alloys. The scales formed at the various sulfidation conditions on both the Alloy

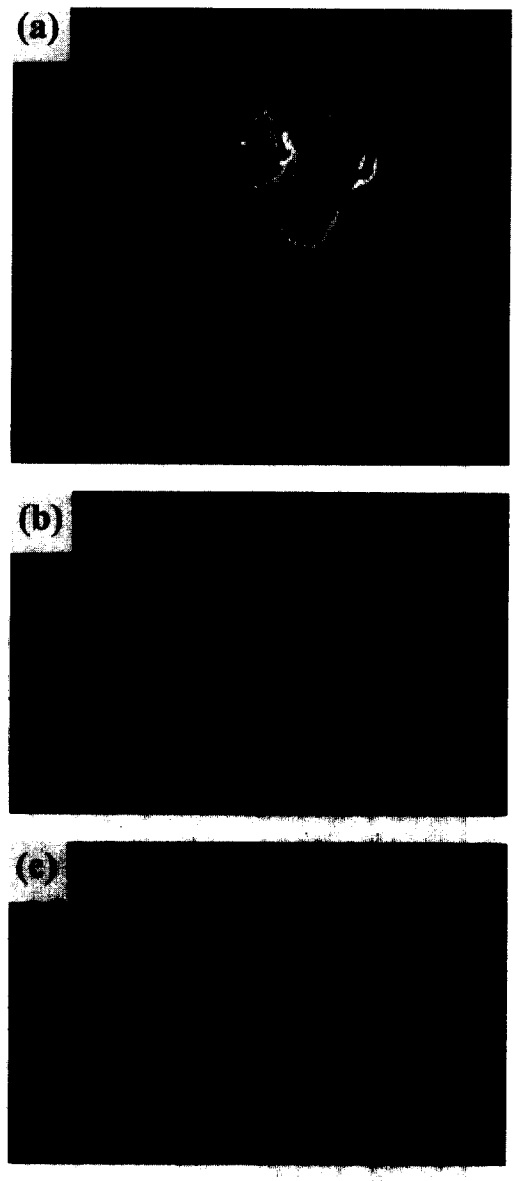

Fig. 5. Typical form of YAl_xO_y oxide (a) and X-ray mapping of yttrium(b) and sulfur(c).

690 and Alloy 690-0.1wt.%Y were analyzed by SEM-EDX. Fig. 7 shows the appearance of oxide that formed on Alloy 690 after 900℃, 6hr sulfidation of flowing Ar-10%CO_2-2%SO_2 gas where relatively uniform, thick and large grained scales were developed throughout the

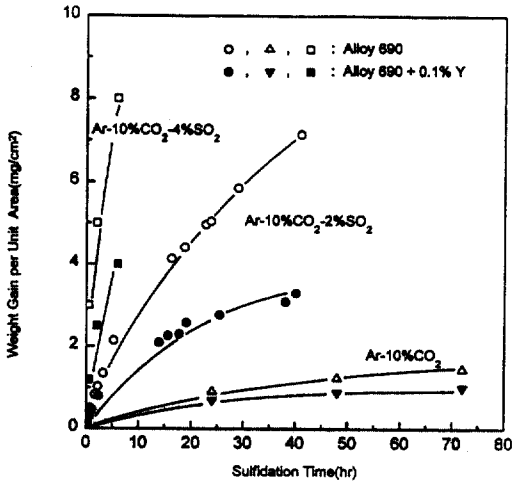

Fig. 6. Isothermal sulfidation rate of Alloy 690 and Alloy690-0.1wt.%Y at 900℃.

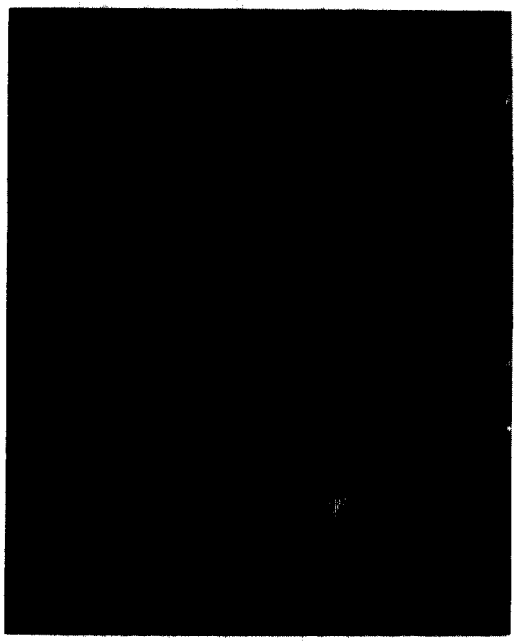

Fig. 7. SEM micrograph of oxide formed on Alloy 690 after 900℃ sulfidation for 6hr.

whole specimen with a small spalled region. Fig. 7 showed that the scale spalled mainly on the grain interior and a thicker oxide developed along the grain boundaries. EDX analysis con-

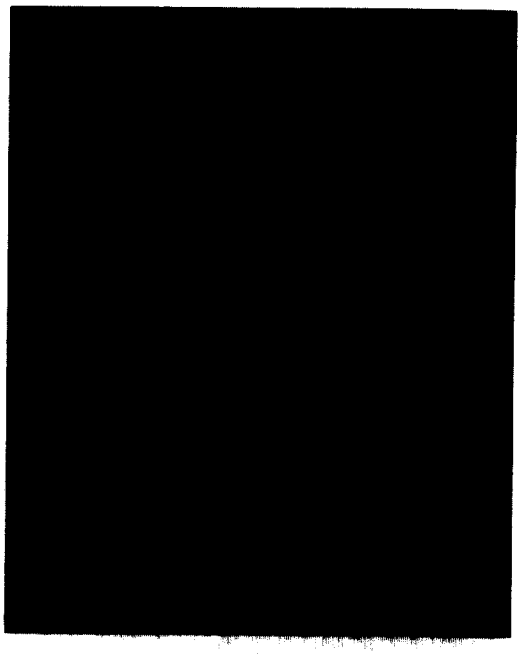

Fig. 8. SEM micrograph of oxide formed on Alloy 690-0.1wt.%Y after 900℃ sulfidation for 6hr.

firmed that the scales were mainly Cr_2O_3 and a small amount of CrS. After a 900℃, 24 hr sulfidation, the appearance of the scale remained unchanged except that there were more scales on the grain boundaries and spallation on the grain interior was observed in the yttrium free alloy.

By contrast, oxide scales of complex shapes were found in the Y containing alloy. Fig. 8 shows the SEM micrograph of oxide formed on Alloy 690-0.1wt.%Y after a 900℃, 6hr sulfidation of flowing Ar-10%CO_2-2%SO_2 gas. The bulk of the surface was covered with a considerably thicker oxide scale which had the same appearance as the yttrium free alloy, but there was a thin non-uniform oxide scale with small grains where yttrium was found. Therefore, it is considered that the formation of a complex oxide scale may be due to the non-uniform distribution of yttrium in the alloy and yttrium

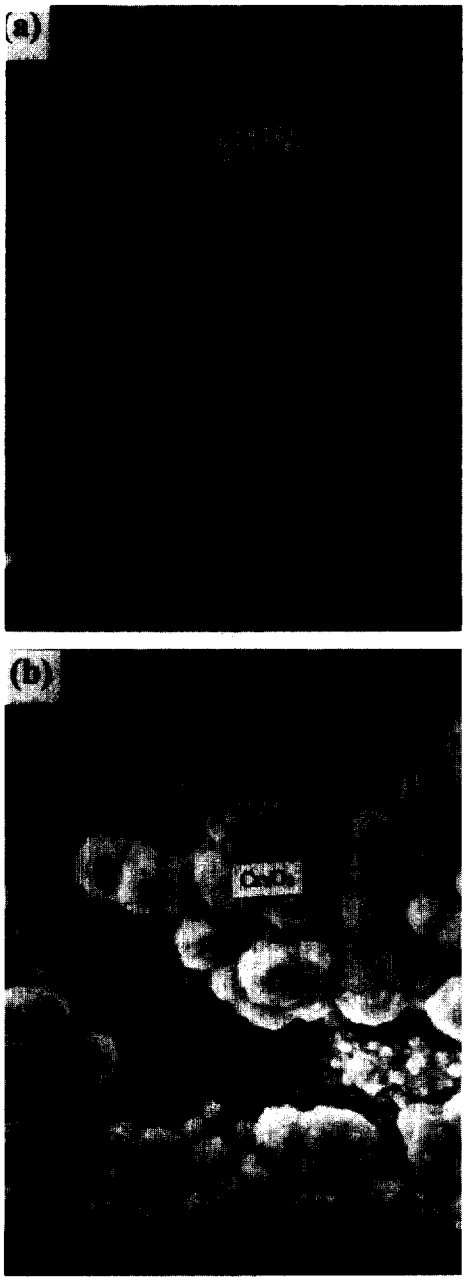

Fig. 9. High magnification of oxide scale spalled. (a) Alloy 690 and (b) Alloy 690+0.1wt.%Y after 900℃, 24hr sulfidation.

acts as a oxide scale refiner. Fig. 9 shows the oxide scale at a high magnification. EDX results show that the thin oxide region with small grain generally contained yttrium of 0.1 to 7wt.% Cr contents in the scale of the yttrium bearing region increased with sulfidation time, from 35wt.% Cr after 6hr sulfidation to 60wt.% Cr after 24 hr sulfidation, implying that the scale formed on the yttrium bearing region was not completely covered with Cr_2O_3. It is probable that oxidation on the yttrium containing region was too sluggish and the scale was still mixed with Cr_2O_3 and (Ni,Fe)O scale, which generally were shown in the very early stage of corrosion.[7] The oxide scale thickness of the yttrium free alloy and the yttrium containing alloy after a 900℃, 24hr sulfidation by SEM were about 5μm and 2μm, respectively. While the scale thickness was relatively uniform in the yttrium free alloy, it was not uniform in the Y bearing alloy.

Sulfidation at higher SO_2 gas content further altered the scale morphology. Fig. 10 is a SEM micrograph of the sulfide scale formed on Alloy 690-0.1wt.% Y after 2 hr sulfidation at 900℃ with a flowing gas of Ar-10%CO_2-4%SO_2. A bi-layered scale was formed on both Alloy 690 and Alloy 690-0.1wt.% Y ; an inner layer of CrS and an outer layer of a mixture of CrS and (Ni,Fe)S which may formed later and would have been surrounded by CrS. Due to the difference of thermal expansion between the CrS and the (Ni,Fe)S scale, the outer scale spalled during cooling. According to the metal-oxygen-sulfur thermodynamic phase stability diagram,[15] the types of scales that formed during sulfidation as well as the sulfidation rate are determined by the ratio of the partial pressures of O_2 and S_2. It is probable that oxidation prevailed up to a 2%SO_2 gas content, while sulfidation prevailed at 4 %SO_2, resulting in changes of

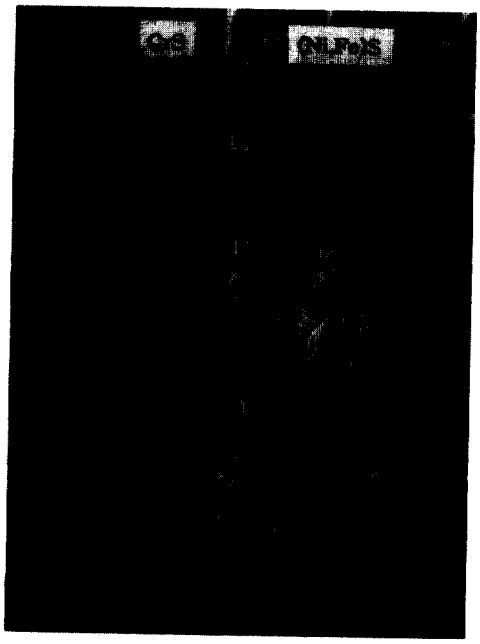

Fig. 10. SEM micrograph of sulfide scale formed on the Alloy 690-0.1wt.%Y after 900℃, 2hr sulfidation in Ar-10CO_2-4SO_2.

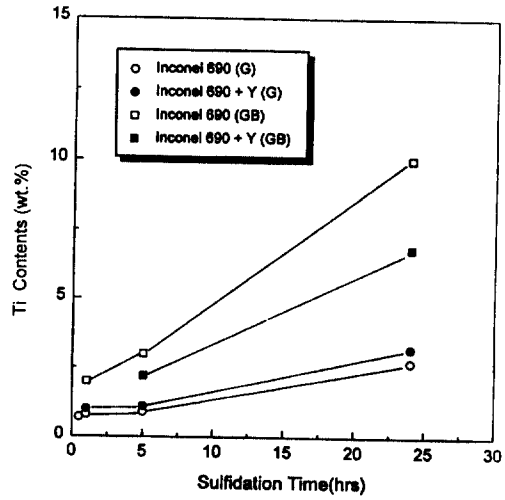

Fig. 11. Relationship between titanium contents and sulfidation time both on grain boundary and in the matrix. G stands for grain and GB stands for grain boundary.

thermodynamically stable phases from Cr_2O_3 to CrS.

It was also found that titanium segregated to both the grain surface and the grain boundaries (Figs. 7 and 8). After 24hr sulfidation, more titanium had segregated toward the grain boundaries in both alloys. Titanium segregation with respect to sulfidation time of both alloys are shown in Fig. 11. It was observed that more titanium segregated onto the surface, and especially into the grain boundaries, in the yttrium free alloy than in the yttrium bearing alloy and that more titanium could be found at the outer scale than the inner scale closely located at scale/metal interface. Two possible models to be able to explain titanium segregation in both alloys are the cation to anion transport mechanism and chromium doping mechanism. In the transport mechanism,[8] it is explained that the segregation of Y^{3+} cations at the grain boundaries reduced either Ti^{3+} or Cr^{3+} flux, thereby reducing the growth rate of the Cr_2O_3 scale. By contrast, Ramanarayanan[9] reported that yttrium in the form of yttrium oxide and titanium can dope, as a donor, into a trivalent oxide, which will decrease the concentration of chromium interstitial defects and thereby suppress chromium transport rate. He also reported experimentally that titanium has little influence on the parabolic growth constant for the chromia growth on the Ni-30Cr-0.5Ti alloy. It is not clear which mechanism is dominant, but it is probable that yttrium, more preferentially than titanium, can block chromium transport, thereby reducing the overall sulfidation rate.

The examples of the yttrium-rich phase intruding into the metal substrate at the CrS/mixed CrS+(Ni,Fe)S interface in spalled areas after a 900℃, 2hr sulfidation of the flowing gas

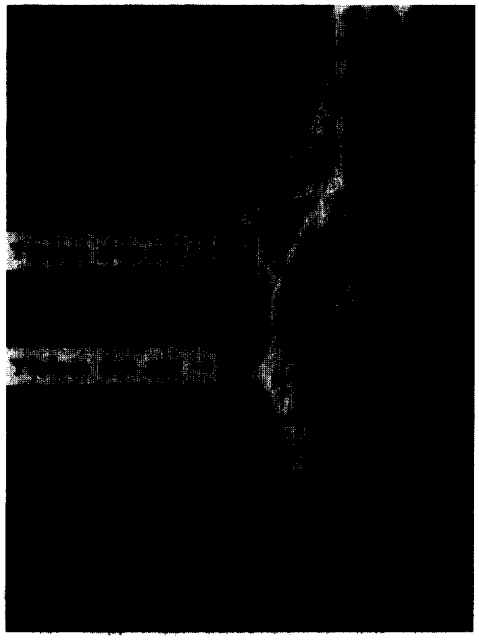

Fig. 12. Examples of the pegging effect by yttrium.

of Ar-10%CO_2-4%SO_2 in the yttrium bearing alloy are shown in Fig. 12, supporting the well-known pegging argument. Zhang et al.[16] recently reported that a few yttrium-rich fibers were found at the metal/oxide interface and a void was formed around the fiber, as if the interface between the fiber and metal acted as a site for vacancy condensation. However, such a void forming around the yttrium-rich fiber was not found in this study. It is probable that the volume fraction of the pegs that was found was too small to protect the scales from spallation completely. Therefore, it was proposed that the sulfidation process in these alloys is a result of several mechanisms operating simultaneously and the role of yttrium strongly relies upon the sulfidation environment and alloy system.

4. Conclusions

Two types of yttrium-rich phases, yttrium precipitated on the grain boundaries and yttrium oxide inclusions in both the matrix and the grain boundaries, were found in this study. It was also found that the microstructure and the recrystallization temperature of both alloys were unchanged, whereas the grain growth and tensile properties slightly changed by a yttrium addition. SEM and EDX analyses showed that yttrium acts as a sulfur getter.

The isothermal sulfidation rate of Alloy 690 was reduced by about a factor of 2 with the addition of 0.1wt.% yttrium. Oxide scale analyses by SEM-EDX showed that Cr_2O_3 with small amount of CrS scales were formed on Alloy 690, whereas more complex scales were formed on Alloy 690-0.1% Y, depending on whether yttrium was present or not on the matrix, due to the non-uniform distribution of yttrium in flowing Ar-10%CO_2-2%SO_2. Small grained oxides were found near the region where yttrium is present implying that yttrium act as a oxide refiner.

Continuous CrS scales were formed on both the yttrium bearing and yttrium free alloys in flowing Ar-10%CO_2-4% SO_2 in the early stage of sulfidation, but after a longer period of sulfidation, a mixed CrS and (Ni,Fe)S outer layer was found. This outer scale created thermal stress during cooling due to the difference of the thermal expansion between CrS and (Ni,Fe)S scale and spallation at these scale interfaces was observed.

More titanium segregated onto the surface, and especially into the grain boundaries of the yttrium free alloy than the yttrium bearing alloy, indicating that yttrium, more preferential-

ly than titanium, can block chromium transport, thereby reducing the overall sulfidation rate. Pegging by yttrium was also found. This result supported that yttrium promotes the formation of oxide intrusion into the metal substrate.

On the subject of improved sulfidation resistance with the presence of yttrium, it was found that yttrium acts as sulfur getter, oxide grain refiner or pegs in this study and believed that more than one mechanism is operative simultaneously and the role of yttrium strongly depends on the sulfidation environment as well as the alloy system.

Acknowledgements

One of authors(CKR) gratefully acknowledges the support of the Korea Science and Engineering Foundation(KOSEF) during the course of this study. They are also grateful to INCO Alloys International Incorporated for supply of the alloy used in this study and for their analyses of the superalloy samples.

References

1. I. H. Kuk et. al., *Research Report KAERI/RR* 1520/94, Korea Atomic Energy Research Institute, (1995).
2. E. Schumann, J. C. Yang and M. J. Graham, *Scripta Mater.*, **34**, 1365 (1996).
3. J. L. Smialck, D. T. Jayne, J. C. Schaeffer and W. H. Murphy, *Thin Solid Films*, **253**, 285 (1994).
4. K. N. Strafford and J. M. Harrison, *Metal-Slag-Gas Reactions and Processes*, 464 (1975).
5. H. J. Grabke, J. F. Norton and F. G. Casteels, *Proc. of a conf. on High Temperature Alloys for Gas Turbine and Other Applications*, 245 (1986).
6. C. S. Giggins and F. S. Pettit, *Metall. Trans.*, 2, 1071 (1971).
7. J. Stringer, B. A. Wilcox and R. I. Jaffee, *Oxid Met.*, **5**, 11 (1972).
8. C. M. Cotell, G. J. Yurek, R. J. Hussey, D. M. Mitchell and M. J. Graham, *Oxid. Met.*, **34**, 173 (1990).
9. T. A. Ramanarayanan, R. Ayer, R. Petkovic-Luton and D. P. Leta, *Oxid. Met.*, **29**, 445 (1988).
10. D. P. Whittle and J. Stringer, *Phil. Trans. Roy. Soc.*, **A295**, 309 (1980).
11. J Stringer, *Mater. Sci. Eng.*, **A120**, 129 (1989).
12. B. Pieraggi and R. A. Rapp, *J. Electrochem. Soc*, **1405**, 2844 (1993).
13. J. G. Smeggil, A. W. Funkenbusch and N. S. Bornstein, *Metall. Trans. A*, **17A**, 923 (1986).
14. A. W. Funkenbusch, J. G. Smeggil and N. S. Bornstein, *Metall. Trans. A*, **16A**, 1164 (1985).
15. J. F. Norton, F. G. Hodge and G. Y. Lai, *Proc. of a conf. on High Temperature Alloys for Gas Turbine and Other Applications*, 167 (1990).
16. Y. Zhang, D. Zhu and D. A. Shores, *Acta Metall. Mater.*, **43**, 4015 (1995).